The Reduced Kinetic Description of Lean Premixed Combustion

A. Liñán†, A. L. Sánchez‡, A. Lépinette†, M. Bollig† and B. Lázaro†

† Departamento de Motopropulsión y Termofluidodinámica, E. T. S. I. Aeronáuticos,
Universidad Politécnica de Madrid, 28040 Madrid, Spain
‡ Area de Mecánica de Fluidos, Departamento de Ingeniería Mecánica,
Universidad Carlos III de Madrid, 28911 Leganés, Spain

ABSTRACT

Lean premixed methane-air flames are investigated in an effort to facilitate the numerical description of CO and NO emissions in LPP (lean premixed prevaporized) combustion systems. As an initial step, the detailed mechanism describing the fuel oxidation process is reduced to a four-step reduced description that employs CO, H_2 and OH as intermediates not following a steady-state approximation. It is seen that, under conditions typical of LPP combustion, the mechanism can be further simplified to give a two-step description, in which fuel is consumed and CO is produced according to the fast overall step $CH_4 + \frac{3}{2}O_2 \rightarrow CO + 2H_2O$, while CO is slowly oxidized according to the overall step $CO + \frac{1}{2}O_2 \rightarrow CO_2$. Because of its associated fast rate, fuel consumption takes place in thin layers where CO, H_2 and OH are all out of steady state, while CO oxidation occurs downstream in a distributed manner in a region where CO is the only intermediate not in steady state. In the proposed description, the rate of fuel consumption is assigned a heuristic Arrhenius dependence that adequately reproduces laminar burning velocities, whereas the rate of CO oxidation is extracted from the reduced chemistry analysis. Comparisons with results obtained with detailed chemistry indicate that the proposed kinetic description, not only reproduces well the structure of one-dimensional flames, including profiles of CO, temperature and radicals, but can also be used to calculate NO emissions by appending an appropriate reduced chemistry description that includes both the thermal and the N_2O production paths. Although methane is employed in the present study as a model fuel, the universal structure of the resulting CO oxidation region, independent of the fuel considered, enables the proposed formulation to be readily extended to other hydrocarbons.

INTRODUCTION

Pollutant emissions have become one of the limiting factors when designing combustion chambers of gas turbine engines. In general, traditional design methodologies, largely based on empirical correlations, fail to provide reliable predictions of CO and NO emissions. With the ever increasing computer power, the numerical computation of the associated reacting flow fields has become a commonly used design tool. For the numerical results to be meaningful, the computations must incorporate adequate models for the turbulent flow field, as well as an accurate representation for the underlying chemistry. The chemistry descriptions currently utilized to predict CO and NO emissions are based on empirically fitted rates, its applicability range being therefore necessarily limited.

A more reliable description can be obtained from systematically reducing the chemical kinetic mechanism, a technique that has been succesfully utilized in the description of both premixed and diffusion flames. A recent work along this line is that of Li *et al.* (1999), who investigated fuel-lean premixed combustion in the limit of slow CO oxidation, reducing the hydrocarbon chemistry to two overall steps: fuel consumption and CO oxidation. For the application investigated, fuel consumption is assumed to be controlled by turbulence, and it is assigned a rate derived from a simple eddy-breakup model, while the rate of CO oxidation is rationally derived by introducing a number of partial-equilibrium and steady-state assumptions for the chemistry description. The authors also assume that NO is mainly produced by the thermal mechanism, providing a simple chemistry formulation that is applied to the calculation of NO emissions from a dual-fuel reciprocating engine, yielding results in excellent agreement with experimental measurements.

Among the different concepts designed to meet the ever more stringent regulations on pollutant emissions, lean premixed prevaporized combustion systems (LPP) are currently subject to intensive research. The present study is concerned with the development of a simplified chemical-kinetic reduced mechanism well suited for the description of combustion in such systems. The conditions of interest here are then preheated fuel-lean mixtures burning at elevated pressures. Since pollutant prediction is a major goal of the reduced mechanism, the needed description for fuel oxidation not only must accurately reproduce flame velocities and temperature distributions, but also concentrations of intermediates such as CO, O, H, and OH. In addition, oxides of nitrogen must be appropriately described by including in the mechanism all relevant production paths.

Our approach is similar to that followed in the unrelated work of Li *et al.* (1999), in that the limit of slow CO oxidation is also incorporated here, giving two overall steps for hydrocarbon oxidation. The resulting rate expressions are however different. On the one hand, fuel consumption is assigned here an Arrhenius rate that, unlike that of Li *et al.* (1999), enables calculations of laminar flames, serving also as starting point in turbulent modelling efforts. On the other hand, we found that some of the approximations used in (Li *et al.*, 1999) when deriving the CO-oxidation rate may lead to non-

negligible errors under some flow conditions. By retaining all these missing effects, our CO-oxidation rate is seen to describe accurately CO and radicals everywhere. In addition, the contribution of the nitrous-oxide path to NO emissions, that was previously neglected in (Li *et al.*, 1999), is seen to be significant under LPP combustion conditions, and is consequently retained here in the nitrogen chemistry.

Although methane is selected as a model fuel in the present analysis, the results are applicable to other hydrocarbons because of the fuel-lean conditions addressed, that is, the resulting reduced mechanism is readily extendible by appropriately changing the fuel consumption rate. In the starting detailed chemistry description we choose to disregard the C_2 chain of fuel oxidation. This chain is known to be important in describing flame structures and burning velocities for sufficiently rich flames (Peters and Rogg, 1993) Since a considerable fraction of CH is created through a reaction path that begins with $C_2H_2 + O \rightarrow CH_2 + CO$, retaining the C_2 species can also be important in describing production of oxides of nitrogen through the so-called prompt mechanism, which involves $CH + N_2 \rightarrow HCN + N$. Here, we are concerned with lean premixed enviroments, in which the prompt mechanism is seen to have only a marginal contribution to NO production. Therefore, in this study the C_2 chain can be neglected altogether, yielding a detailed mechanism for fuel oxidation that contains 57 elementary reactions and 17 species. Details of the mechanism and its associated rates, which are largely taken from the recent recommendations of the CEC group (Baulch*et al.*, 1994), are presented for brevity elsewhere (Liñán *et al.*, 1999). The nitrogen chemistry, which does not influence the fuel-oxidation process because of the very slow rates of its associated reactions, can be similarly simplified by retaining only the thermal and N_2O paths of NO production, thereby limiting the necessary description to 46 elementary steps with 9 nitrogen-containing species (Liñán *et al.*, 1999).

Insight into the complex chemical processes may only be obtained by accounting for detailed chemistry and transport, a task that is nowadays feasible with reasonable effort in computations of one-dimensional laminar flames. Results corresponding to numerical computations of planar flames will be used here in the development and subsequent tests of the reduced chemistry description. The "FlameMaster" code (Pitsch and Bollig, 1994) previously used for instance by Hewson and Bollig (1996), is utilized in the detailed calculations. Different values of the pressure, p, and of the temperature and equivalence ratio of the reactant mixture, T_u and ϕ, were considered in the computations, with conditions covering in particular those of aeronautical applications. Thus, to represent typical cruise conditions, calculations were performed with $p = 18$ bar, $T_u = 800$ K and $\phi = 0.6$, while the case $p = 40$ bar, $T_u = 900$ K and $\phi = 0.6$ was selected as characteristic of takeoff conditions.

The structure of the paper is as follows. A four-step mechanism for CH_4 oxidation under lean premixed gas-turbine combustion conditions is derived first, and is further reduced in the following section to finally give a two-step mechanism. The starting nitrogen chemistry description is next reduced to two global reactions, that simplify to a single overall step when nitrous oxide is assumed to follow a steady-state approximation. Validation of the reduced kinetics through extensive comparisons with results of detailed chemistry is given next. Finally, a general formulation for the energy and species conservation equations based on the reduced chemistry description is presented.

THE FOUR-STEP REDUCED MECHANISM FOR CH_4 OXIDATION

Previous studies have shown that a four-step reduced description, including CO, H_2 and H as intermediate species out of steady state, suffices to describe most aspects of lean and stoichiometric premixed flames (Peters and Rogg, 1993). Numerical calculations incorporating such mechanisms accurately reproduce for instance laminar propagation velocities, with errors that are typically smaller than a few percent over a wide range of flow conditions. A three-step mechanism, that follows from introducing a steady-state assumption for H, and also a two-step mechanism, obtained by incorporating a partial-equilibrium approximation for the water-gas shift reaction $CO + OH \overset{17}{\rightleftharpoons} CO_2 + H$, have also been proposed (Peters and Williams, 1987). Although these reduced descriptions capture well the flame structure, they lead to fairly large errors in flame propagation velocities, so that a four-step mechanism is generally accepted as the minimal chemistry description for numerically computing premixed combustion (Peters and Rogg, 1993).

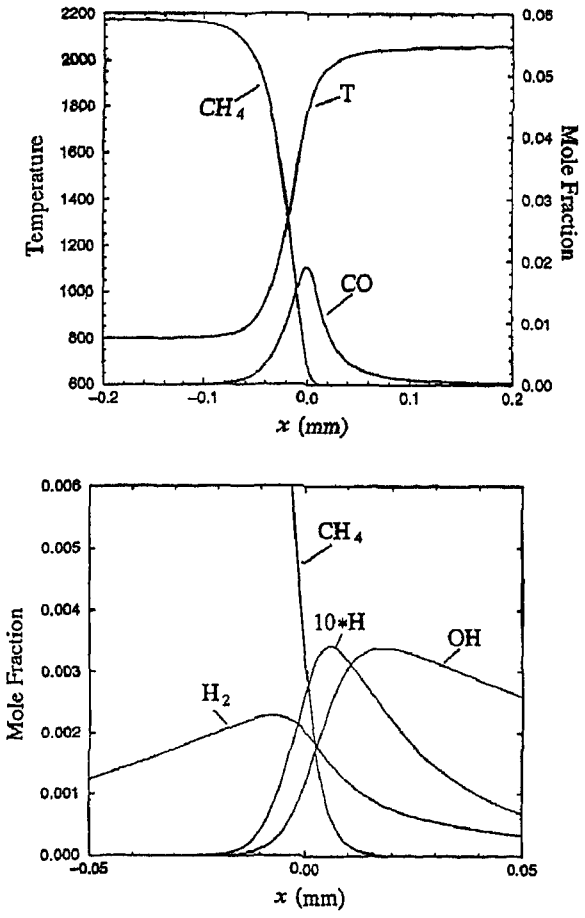

Figure 1: Temperature and species mole fractions across a laminar methane-air flame with $p = 18$ bar, $T_u = 800$ K and $\phi = 0.6$

The above considerations suggest that a four-step mechanism is also an adequate first step in reducing the kinetic description of LPP systems. Because of the particular characteristics of the combustion systems we study here, namely, preheated lean mixtures burning at relatively high pressures, modifications to the previous reduced kinetic mechanisms (Peters and Rogg, 1993) can be expected. To illustrate features of the resulting flames, profiles of species and temperature corresponding to a nonradiating premixed flame with $p = 18$ bar, $T_u = 800$ K and $\phi = 0.6$ are shown in Fig. 1. The computations, which are performed with the detailed chemistry description previously discussed, reveal for instance that OH mole fractions are an order of magnitude larger that those of H, suggesting that OH is the dominant H_2-O_2 radical. Therefore, although previous reduced chemical-kinetic mechanisms of methane combustion prefer to employ H as representative for the radical pool, under LPP combustion conditions it seems appropriate to introduce a steady-state assumption for H atoms, and replace H by OH as the H_2-O_2 radical out of steady state.

Following this finding, we choose here to introduce steady-state approximations for all intermediates except CO, H_2 and OH. The procedure yields the four-step reduced chemical-kinetic mechanism

$$\begin{aligned} CH_4 + 2OH &\rightarrow CO + H_2O + 2H_2, && \text{(I')} \\ H_2 + O_2 &\rightleftharpoons 2OH, && \text{(II')} \\ 2OH + H_2 &\rightleftharpoons 2H_2O, && \text{(III')} \\ CO + H_2O &\rightleftharpoons CO_2 + H_2. && \text{(IV')} \end{aligned}$$

As can be seen, fuel consumption occurs according to step I' in a process that involves radical removal. Step II' is the oxygen-consumption step, which produces radicals through the hydrogen-oxygen chain, and step III' represents radical recombination. The final step IV' is the water-gas shift that converts the CO produced by step I' to CO_2.

Although several elementary reactions contribute to the rate of global steps I'-IV', retaining only a few contributors to each step is seen to provide a reasonably accurate description. If for instance an error of 10 % is accepted in the calculation of laminar flame velocities, then an appropriate set of simplified global rates (moles per unit volume per unit time) is found to be

$$\begin{aligned} \omega_{I'} &= k_{34f}[CH_4][H] + k_{36f}[CH_4][OH], \\ \omega_{II'} &= k_{1f}[O_2][H] - k_{1b}[O][OH], \\ \omega_{III'} &= k_{6f}[M][O_2][H] - k_{6b}[M][HO_2], \\ \omega_{IV'} &= k_{17f}[CO][OH] - k_{17b}[CO_2][H], \end{aligned} \qquad (1)$$

where $[i]$ denotes the concentration of chemical species i, M representing a third body, and k_{jf} and k_{jb} the specific reaction-rate constants in the forward and backward directions for the elementary reactions $CH_4 + H \overset{34}{\rightleftharpoons} CH_3 + H_2$, $CH_4 + OH \overset{36}{\rightleftharpoons} CH_3 + H_2O$, $O_2 + H \overset{1}{\rightleftharpoons} O + OH$, $O_2 + H + M \overset{6}{\rightleftharpoons} HO_2 + M$ and $CO + OH \overset{17}{\rightleftharpoons} CO_2 + H$. If the reverse rate of reaction 6 were not included in the mechanism, then the resulting equilibrium values of all intermediates for the reduced mechanism I'-IV' would be zero, thereby potentially introducing significant errors in predictions of CO and NO formation. We therefore choose to retain this rate in the mechanism for increased accuracy.

Expressions for the different reaction-rate constants are given in cm^3/mole/second by $k_{34f} = 1.300 \times 10^4\, T^{3.00} \exp(-4041/T)$, $k_{36f} = 1.600 \times 10^7\, T^{1.83} \exp(-1395/T)$, $k_{1f} = 9.756 \times 10^{13} \exp(-7469/T)$, $k_{1b} = 1.445 \times 10^{13} \exp(-352/T)$, $k_{6f}[M] = 1.82 \times 10^{16}\, T^{-1.80} p$, $k_{6b} = 5.058 \times 10^{18}\, T^{-0.80} \exp(-23574/T)$, $k_{17f} = 4.400 \times 10^6\, T^{1.50} \exp(373/T)$ and $k_{17b} = 1.270 \times 10^9\, T^{1.50} \exp(-11872/T)$, where T and p are expressed in kelvins and atmospheres, respectively. Note that a third-body efficiency equal to 0.4 has been used above when writing the expression for [M], although the more complicated equation [M]=(0.6 [H_2] + 0.4 [N_2] + 0.44 [H_2O]+ 0.4 [O_2] + 1.5 [CO_2] + 3.0 [CH_4]+ 1.0 [OTHERS]) was actually incorporated in the calculations for increased accuracy. Suitable simplified steady-state expressions for the concentrations of H and O, necessary in evaluating Eq. 1, can be obtained by assuming partial equilibrium of reactions $H_2 + OH \overset{3}{\rightleftharpoons} H_2O + H$ and $OH + OH \overset{4}{\rightleftharpoons} H_2O + O$ to give

$$[H] = K_3[H_2][OH]/[H_2O] \qquad (2)$$

and

$$[O] = K_4[OH]^2/[H_2O], \qquad (3)$$

where $K_3 = 0.227 \exp(7614/T)$ and $K_4 = 0.0966 \exp(8573/T)$ are equilibrium constants. Similarly, the concentration of hydroperoxyl radicals needed to evaluate the backward rate of III' can be obtained from the truncated steady-state expression

$$[HO_2] = \frac{k_{6f}[M][O_2][H] + k_{11b}[O_2][H_2O]}{k_{6b}[M] + k_{11f}[OH]}, \qquad (4)$$

where the rate constants $k_{11f} = 2.891 \times 10^{13} \exp(253/T)$ and $k_{11b} = 3.069 \times 10^{14} \exp(-36083/T)$ (cm^3/ mole/second) correspond to the reaction $HO_2 + OH \overset{11}{\rightleftharpoons} H_2O + O_2$.

THE TWO-STEP REDUCED MECHANISM FOR CH_4 OXIDATION

The Limit of Slow CO Oxidation

CO-oxidation is the slowest of the four chemical processes represented by I'-IV' (Bui-Pham *et al.*, 1992). To illustrate this, one can use Eq. 1 to give the characteristic chemical-time ratios $t_{I'}/t_{IV'} = k_{17f}/(k_{34f}K_3)$, $t_{II'}/t_{IV'} = k_{17f}/(k_{1f}K_3)$ and $t_{III'}/t_{IV'} = k_{17f}/(k_{6f}[M]K_3)$. Evaluating the above estimates at the temperatures and pressures typical of gas-turbine combustion yields the scaling law $t_{I'} \sim t_{II'} \sim t_{III'} \ll t_{IV'}$ (for instance, at $T = 1700$ K and $p = 30$ atm, $t_{I'}/t_{IV'} = 0.01$, $t_{II'}/t_{IV'} = 0.016$ and $t_{III'}/t_{IV'} = 0.022$). As a direct consequence of these relative scalings we find the flame structure observed in Fig 1; fuel consumption followed by radical branching and radical recombination all occur in a thin layer that exhibits small concentrations of H_2 and radicals, while CO-oxidation is much slower, and consequently occurs

in a distributed manner in a downstream region where in the first approximation $[CH_4]=0$ and both H_2 and OH maintain steady state (Bui-Pham *et al.*, 1992). Because of fast radical removal through reaction I', all chemical activity is frozen in the preheat zone upstream from the fuel-consumption layer (Peters and Williams, 1987). Note that the relatively fast rate of radical recombination (represented by the condition $t_{III'}/t_{IV'} \ll 1$), which leads to a steady-state approximation for H_2 in the CO-oxidation region, is a consequence of the existing high-pressure conditions, which enhance H_2 consumption through reaction III'. Therefore, while the H_2 mole fraction is typically comparable in magnitude to the CO mole fraction in atmospheric flames, it exhibits in this high-pressure case a peak value an order of magnitude smaller than that of CO.

The overall step occuring in the thin fuel-consumption layer can be obtained by eliminating H_2 and OH by linear combinations of I'–III' to give

$$CH_4 + \frac{3}{2}O_2 \rightarrow CO + 2H_2O. \qquad (I)$$

On the other hand, incorporating the steady states of H_2 and OH into step IV' by linear combinations with steps II' and III' provides the global CO-oxidation step

$$CO + \frac{1}{2}O_2 \rightleftharpoons CO_2. \qquad (II)$$

In the thin fuel-consumption layer where fuel attack by radicals takes place, giving as a result the overall reaction I, neither OH nor H_2 follow a steady-state approximation. Therefore, utilizing $\omega_I = \omega_{I'}$ for the rate of reaction I, with the radical concentrations evaluated from appropriate steady-state expressions, leads to flame propagation velocities with errors of order unity. As previoulsy discussed, this characteristic precludes in principle the use of reduced mechanisms with less than four steps, and requires the detailed description of the very thin fuel-consumption layer if flame propagation velocities are to be reproduced. To circumvent this difficulty, we propose to represent ω_I by an Arrhenius law of the form of the form

$$\omega_I = B[CH_4]\exp\left(-\frac{E}{R^oT}\right), \qquad (5)$$

where R^o is the universal gas constant. As explained below, the values of the activation energy, $E = 57400$ cal/mole/K, and of the preexponential factor, $B = 4.8 \times 10^{12}$ s^{-1}, were chosen to adequately reproduce the steady flame propagation velocity under a wide range of conditions. On the other hand, the rate of reaction II is given by

$$\omega_{II} = \omega_{IV'} = k_{17f}[CO][OH] - k_{17b}[CO_2][H]. \qquad (6)$$

As shown below, the CO-oxidation rate given in Eq. 6 describes accurately the nonequilibrium evolution of the CO concentration, as well as its associated radical pool (through appropriate steady-state expressions), downstream from the fuel-consumption layer, with the failure of the steady-state approximations for OH and H_2 within the thin fuel-consumption layer having only a very limited effect.

Steady-State Expressions for H_2 and OH

To completely define the rate given in Eq. 6, the concentrations of OH and H appearing in Eq. 6 must be calculated in terms of the concentrations of O_2, CO, CO_2 and H_2O and temperature. In the CO-oxidation region. the corresponding steady-state equations for H_2 and OH with $[CH_4] = 0$, $-\omega_{II'} - \omega_{III'} + \omega_{IV'} = 0$ and $2\omega_{II'} - 2\omega_{III'} = 0$, can be solved to give the expression

$$[H_2] = K_3^{-1}[O_2]^{-1}\alpha_1\{(K_4/K_1)[OH]^2 + \frac{1}{2}(k_{17f}/k_{1f})[CO][H_2O]\}, \qquad (7)$$

together with the fourth-order polynomial

$$a_4[OH]^4 + a_3[OH]^3 + a_2[OH]^2 + a_1[OH]^1 + a_0 = 0, \qquad (8)$$

where we have introduced the coeficients

$$\begin{aligned} a_4 &= -(K_4k_{11f}/K_1)[1-\alpha_1(1-\gamma)], \\ a_3 &= -(K_4k_{6b}/K_1)[1-\alpha_1][M], \\ a_2 &= \frac{1}{2}\alpha_1(k_{17f}k_{11f}/k_{1f})(1-\gamma)[CO][H_2O], \qquad (9) \\ a_1 &= \frac{1}{2}\alpha_1(k_{17f}k_{6b}/k_{1f})[M][CO][H_2O], \\ a_0 &= (k_{6b}k_{11b}/k_{1f})[M][H_2O]^2[O_2]. \end{aligned}$$

and the functions

$$\alpha_1 = \left(1 + \frac{1}{2}\frac{k_{17b}}{k_{1f}}\frac{[CO_2]}{[O_2]}\right)^{-1} \qquad (10)$$

and

$$\gamma = k_{6f}[M]/k_{1f}. \qquad (11)$$

Once Eq. 8 is solved for [OH], one can use Eq. 7 to compute $[H_2]$ and Eqs. 2 and 3 to calculate [H] and [O].

Expressing [OH] through the polynomial given in Eq. 8 is a necessary complication if one wants to accurately describe the chemical equilibrium state, as it is especially desirable in configurations with non-negligible NO production in the postflame region. The simpler explicit steady-state expressions

$$[H_2] = \frac{1}{2}\frac{k_{17f}\alpha_2}{k_{6f}[M]K_3}\frac{[H_2O][CO]}{[O_2]} \qquad (12)$$

and

$$[OH] = \left(\frac{1}{2}\frac{k_{17f}K_1(1-\gamma)\alpha_2}{k_{6f}[M]K_4}\right)^{1/2}[H_2O]^{1/2}[CO]^{1/2}, \qquad (13)$$

where

$$\alpha_2 = \left(1 + \frac{1}{2}\frac{k_{17b}}{k_{6f}[M]}\frac{[CO_2]}{[O_2]}\right)^{-1}, \qquad (14)$$

which are obtained by neglecting the reverse of reaction III', are however a very good approximation in the initial part of the CO-oxidation region. Equations 12 and 13 can be utilized to express 6 in the compact form

$$\omega_{II} = \left(\frac{k_{17f}^3K_1(1-\gamma)\alpha_2^3}{2k_{6f}[M]K_4}\right)^{1/2}[H_2O]^{1/2}[CO]^{3/2}, \qquad (15)$$

as a simplified expression for the CO-oxidation rate corresponding to the limit of irreversible radical recombination. It will be shown below that this alternative description becomes increasingly inaccurate as the CO concentration decreases, giving in particular [CO]=[H_2]=[OH]=0 (and also [H]=[O]=0 by virtue of Eqs. 2 and 3) as the equilibrium state obtained as solution of $\omega_{II} = 0$. This is the limitiation that precludes the use of Eq. 15 in systems with nonnegligible postflame NO production. It is worth remarking that the CO oxidation rate employed in the analysis of Li *et al.* (1999) differs from that given in Eq. 15 in that the backward rate of reaction 17 is neglected, and the rate of the branching reaction 1f is assumed to be much faster than that of the recombination reaction 6f, thereby yielding an even simpler rate expression with $\alpha_2 = 1$ and $\gamma = 0$.

Radical Consumption by Fuel Attack

As previously explained, radical removal through fuel attack ensures a chemically frozen preheat region where CO oxidation does not occur. To incorporate this important effect, which is not reproduced by the present model due to the choice for the fuel-consumption rate given in Eq. 5, an appropriate cutoff must be incorporated in Eq. 6. To guide the selection of this cutoff, it is instructive to momentarily assume that OH maintains steady state in the fuel-consumption layer. Solving for $-2\omega_{I'} + 2\omega_{II'} - 2\omega_{III'} = 0$ with the reverse of reaction III' neglected and with reaction 34f assumed to be faster than 36f yields

$$[OH] = \left\{\frac{K_1K_3}{K_4}(1-\gamma)[O_2][H_2]\right\}^{1/2} \times \left(1 - \frac{k_{34f}[CH_4]}{(1-\gamma)k_{1f}[O_2]}\right)^{1/2}. \quad (16)$$

Observation of the last term in brackets in this equation reveals that radical depletion occurs when the fuel concentration increases to a cutoff value given by

$$[CH_4]_c = (1-\gamma)k_{1f}[O_2]/k_{34f}. \quad (17)$$

This consideration suggests that the effect of radical consumption by fuel attack can be incorporated in the model in a straightforward manner by multiplying the OH concentration obtained from Eq. 8 (or from Eq. 13 if irreversible radical recombination is assumed) by the expression $(1-[CH_4]/[CH_4]_c)^{1/2}$ appearing in Eq. 16. As discussed by Swaminathan and Bilger (1997), this first option introduces complications in the numerical treatment of the problem; the resulting OH profile abruptly decreases to zero, exhibiting a nonzero gradient at the depletion point. In selecting an alternative multiplicative factor, different smooth functional forms, and also different cutoff fuel concentrations with the effect of reaction 36f included, were investigated. The computations of laminar flames showed that the results were quite insensitive to the cutoff selection. Among the different options that provide radical profiles smoothly decaying to zero across the fuel consumption layer, the simple multiplicative factor $(1+\frac{1}{2}[CH_4]/[CH_4]_c)^{-1}$ with $[CH_4]_c$ given in Eq. 17, which in particular reduces to that appearing in Eq. 16 when $[CH_4]/[CH_4]_c \ll 1$, is chosen here for the computations shown in the paper.

THE REDUCED MECHANISM FOR NO PRODUCTION

Introduction of steady-state assumptions for NH_2, HNO, NH, N_2H, NO_2 and N reduces the description of the nitrogen chemistry to the two overall steps

$$N_2 + O_2 \rightarrow 2NO \quad (NI)$$

and

$$N_2 + \frac{1}{2}O_2 \rightarrow N_2O. \quad (NII)$$

The rates of these two global recations are given by

$$\omega_{NI} = k_{N11b}[H][N_2O] + k_{N12b}[OH][N_2] + k_{N18b}[O][N_2] + k_{N25f}[O][N_2O] \quad (18)$$

and

$$\omega_{NII} = -k_{N11b}[H][N_2O] - k_{N21b}[H][N_2O] - k_{N23f}[N_2O][M] + k_{N23b}[N_2][O][M] - k_{N24f}[N_2O][H] - k_{N25f}[O][N_2O]. \quad (19)$$

In these rate expressions, only those elementary reactions that give a nonnegligible contribution have been retained, namely, $H + N_2O \overset{N11b}{\rightarrow} NO + NH$, $N_2 + OH \overset{N12b}{\rightarrow} NO + NH$, $N_2 + O \overset{N18b}{\rightarrow} NO + N$, $N_2O + H \overset{N21b}{\rightarrow} N_2H + O$, $N_2O \overset{N23}{\rightleftharpoons} N_2 + O$, $N_2O + H \overset{N24f}{\rightarrow} N_2 + OH$ and $N_2O + O \overset{N25f}{\rightarrow} 2NO$. The associated reaction-rate constants are given in cm^3/mole/second by $k_{11b} = 1.455 \times 10^{17}\ T^{-0.45} \exp(-17561/T)$, $k_{12b} = 1.834 \times 10^{14}\ T^{-0.23} \exp(-49194/T)$, $k_{18b} = 1.809 \times 10^{14} \exp(-38610/T)$, $k_{21b} = 5.500 \times 10^{18}\ T^{-1.06} \exp(-23815/T)$, $k_{24f} = 2.230 \times 10^{14} \exp(-8432/T)$ and $k_{25f} = 6.620 \times 10^{13} \exp(-13351/T)$. The rate of the unimolecular reaction 23 follows a Lindemann description with low-pressure constants given in cm^3/mole/second by $k_{0f} = 9.000 \times 10^{14} \exp(-28506/T)$ and $k_{0b} = 1.103 \times 10^{13} \exp(-8828/T)$ and with high-pressure constants given in (cm^3/mole)^2/second by $k_{\infty f} = 1.260 \times 10^{12} \exp(-31513/T)$ and $k_{\infty b} = 1.545 \times 10^{10} \exp(-11835/T)$. As previously mentioned, the nitrogen chemistry is very slow, so that the amount of radicals and N_2 consumed through NO production is insignificant. To evaluate Eqs. 18 and 19 one can consequently use the concentrations of H, O and OH determined from Eqs. 2, 3 and 8, and neglect N_2 consumption altogether.

In previous analyses of NO_x emissions (Hewson and Bollig, 1996), the intermediate N_2O is also assumed to maintain steady state, an approximation that is valid sufficiently far downstream from the flame. The mechanism then simplifies to the single overall step NI, with the concentration of N_2O appearing in Eq. 18 evaluated from its steady-state expression, which can be computed in this case by equating to zero Eq. 19 to yield

$$[N_2O] = k_{N23b}[N_2][O][M] / \{(k_{N11b} + k_{N21b} + k_{N24f})[H] + k_{N23f}[M] + k_{N25f}[O]\}. \quad (20)$$

An approximation of this type was seen to be adequate for diffusion flames (Hewson and Bollig,

1996), and will be shown to also provide reasonably accurate results for NO production under most conditions, with overpredictions being always relatively small.

PERFORMANCE OF THE REDUCED KINETICS

The reduced kinetics proposed here is now used to compute one-dimensional laminar flames under different conditions. As previously mentioned, the simplicity of the flowfield configuration selected enables also calculations with detailed chemistry, and the results of the two approaches can then be mutually compared. In comparing both sets of results, one should bear in mind that a detailed transport description (Pitsch and Bollig, 1994) was utilized in the detailed chemistry calculations, while unity Lewis numbers for all chemical species not following a steady-state approximation was assumed for simplicity in the reduced-chemistry computations. Although these preliminary tests show excellent agreement between the results of the reduced mechanism and those of the detailed chemistry, further comparisons, including the effect of strain together with unsteady and multidimensional effects, would be necessary to guarantee the validity of the reduced kinetic description.

Flame Propagation Velocity

An important characteristic of laminar premixed flames, often used as a global performance test for reduced mechanisms, is the flame propagation velocity, u_l. Because of its anticipated relevance in computations of gas-turbine combustion, an accurate description of u_l, through appropriate selection of the parameters E and B of the fuel-consumption rate, emerges as an indispensable condition in developing our reduced kinetic description.

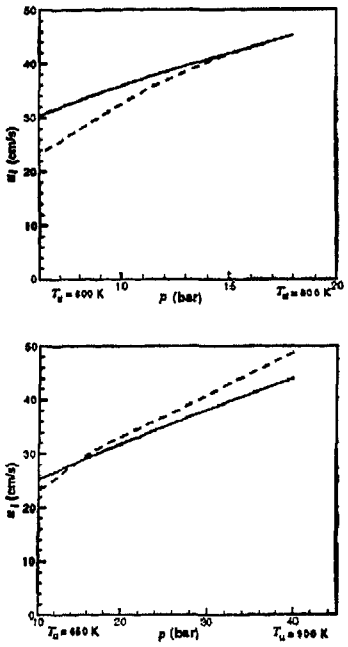

Figure 2: The flame propagation velocity for $\phi = 0.6$ as obtained with detailed chemistry description (solid lines) and with the reduced kinetics (dashed lines).

In general, for a given pressure, p, and given equivalence ratio and temperature of the reactant mixture, ϕ and T_u, there exist an infinite number of pairs of values (E,B) for which the reduced kinetics reproduces the exact value of u_l obtained with detailed chemistry. It is easy to see that, imposing the values of u_l corresponding to two different sets of representative flowfield conditions would in principle suffice to determine E and B. This constitutes a valid strategy in selecting E and B, provided that the selected pair also reproduces with acceptable accuracy the right value of u_l when conditions of temperature, pressure or composition are varied. Alternatively, one could concentrate on a single set of conditions corresponding to a particular application of interest, and find E and B by imposing the value of u_l and considering an additional condition, which could for instance be extracted by studying the flame behavior under strain. This variant would then result in values of E and B that change with the flowfield conditions, so that dependences on mixture composition and fresh-mixture temperature associated to local nonuniformities should in principle be taken into account in the numerical calculation of gas-turbine combustors, thereby complicating the numerical procedure.

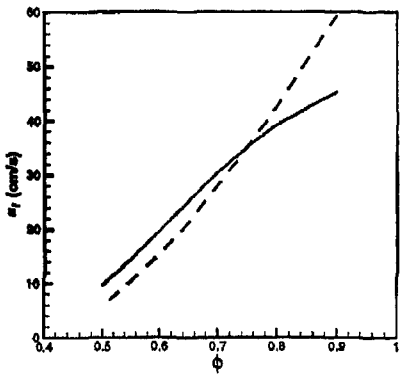

Figure 3: The flame velocity propagation as a function of the equivalence ratio for $p = 7$ bar and $T_u = 520$ K as obtained with detailed chemistry (solid lines) and with the reduced kinetics (dashed lines).

The results presented here correspond in particular to the values $E = 57400$ cal/mole/K and $B = 4.8 \times 10^{12}$ s^{-1}, a selection that reproduces accurately the flame propagation velocity for varying conditions of mixture composition, temperature and pressure, with errors in u_l being typically smaller than 20 %. This is illustrated in Figs. 2 and 3, where the value of u_l obtained with the reduced mechanism is compared to that obtained with detailed chemistry. Figure 2 considers the effect of pressure and temperature for a mixture with $\phi = 0.6$. Beginning with conditions typical of cruise ($p = 18$ bar and $T_u = 800$ K) and takeoff ($p = 40$ bar and $T_u = 900$ K) operations, a decreasing value of p is considered, with the corresponding value of T_u being calculated as that of a polytropic compression of the same initial mixture. Observation of this figure indicates that the reduced kinetics captures the decrease in flame velocity, although the results show a stronger dependence on pressure variations

than that of the detailed chemistry calculations.

A similar agreement is found for the dependence of the flame propagation velocity on the mixture composition. This is investigated in Fig. 3, where we plot the variation of u_l with equivalence ratio for a lean mixture initially at $T_u = 520$ K burning at $p = 7$ bar. Since the reduced kinetics was specifically developed to reproduce combustion in lean enviroments, noticeable departures can be seen as stoichiometric conditions are approached. Nevertheless, the reduced mechanism produces good accuracy over the range of conditions studied.

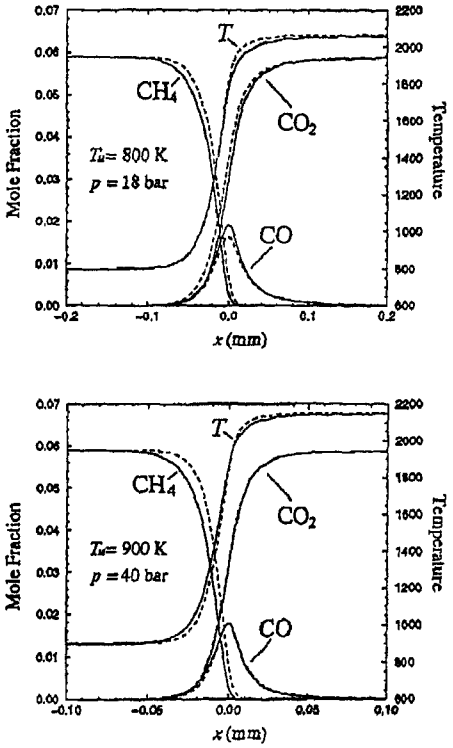

Figure 4: Main species and temperature profiles for $\phi = 0.6$ as obtained with the detailed chemistry description (solid lines) and with the reduced kinetics (dashed lines).

Flame Structure

The characteristic flame structure corresponding to the reduced two-step model is shown in Fig. 4, along with the results of the detailed chemistry calculations. For the mutual comparisons of the results of the two approaches, the distance across the flame x is measured from the location where the CO profile reaches its peak value. This criterion, adopted hereafter for all profile comparisons shown in this paper, removes the arbitrariness associated with the translational invariance of the planar flame. Adoption of a different origin for x, e.g., the location where the value of the fuel concentration decreases to half of its initial value, would result in a small relative translation of the different profiles by an amount of the order of the fuel-consumption layer thickness.

As can be observed in Fig. 4, there exists good agreement in profiles of main species and temperature. In particular, the two-step model adequately reproduces the shape of the CO profile, with peak values differing only by a small amount in the two cases considered. This agreement is further illustrated in Fig. 5(a)-(b), where a logarithmic scale is utilized to show how the proposed formulation remains accurate as equilibrium is approached downstream from the flame. As can be seen in Fig. 5(c)-(h), the agreement extends to profiles of OH, O and H, with the two-step model capturing both the peak concentration and the profile evolution towards equilibrium. In particular, the radical profiles peak slightly downstream from the location of maximum CO concentration. This characteristic, that follows from the inner structure of the fuel-consumption layer (Peters and Williams, 1987), is accurately reproduced by the two-step model through the introduction of radical consumption by fuel attack (the cutoff criterion previously discussed).

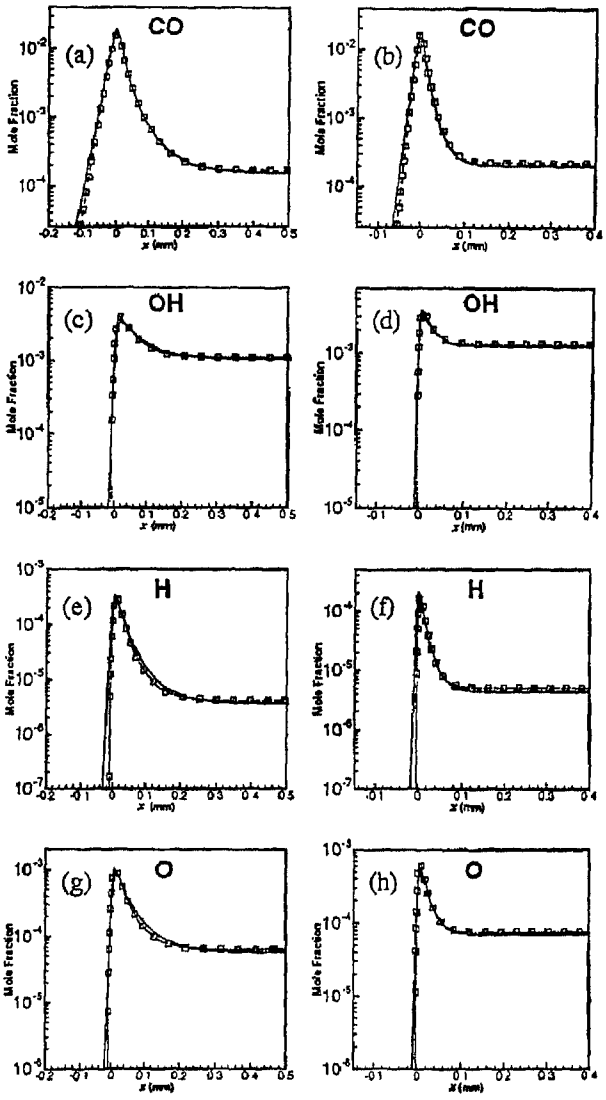

Figure 5: Mole fractions of relevant intermediates as obtained with detailed chemistry (solid lines) and with the reduced kinetics (symbols) for $p = 18$ bar, T_u =800 K and $\phi = 0.6$ (left-hand-side plots) and for $p = 40$ bar, T_u =900 K and $\phi = 0.6$ (right-hand-side plots)

Another point of interest concerns the results corresponding to $p = 40$ bar and $T_u = 900$ K, a case

for which the flame velocity calculated with reduced kinetics ($u_l = 48.80$ cm/s) is larger than that calculated with detailed chemistry ($u_l = 44.02$ cm/s). As can be seen, this discrepancy does not translate into a very large error when calculating the flame structure, suggesting that the inaccuracies in u_l displayed in Figs. 2 and 3 are within an acceptable margin.

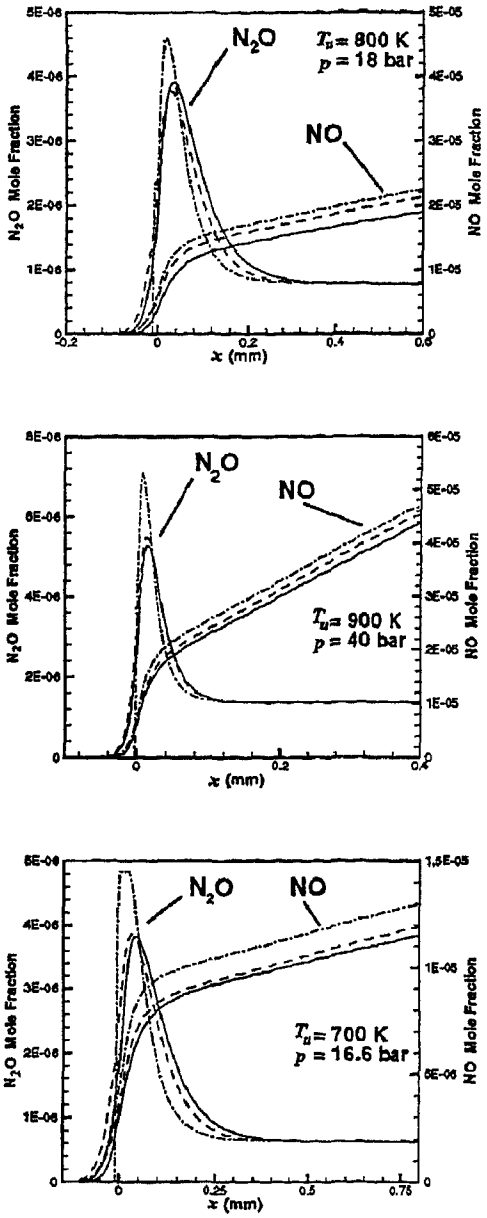

Figure 6: The profiles of NO and N_2O mole fractions for $\phi = 0.6$ as obtained with detailed chemistry (solid lines), with the complete reduced kinetics (dashed lines) and with the reduced kinetics with N_2O in steady state (dot-dashed lines).

Oxides of Nitrogen

Profiles of NO and N_2O mole fractions across the flame obtained with the reduced kinetics are compared in Fig. 6 with detailed-chemistry results. The plot reveals the existence of an initial region of rapid NO growth associated with superequilibrium radical concentrations, followed by a long tail with constant NO-production rate. As can be seen, with the accurate profiles of temperature and radicals determined with the reduced chemistry of fuel oxidation, both regions are accurately computed with the reduced nitrogen chemistry NI-NII.

The accuracy of the steady-state assumption for N_2O is also analyzed in Fig. 6. As can be observed, although the N_2O steady-state profile falls below that of the detailed calculations across the initial and final sections of the flame, it shows an intermediate peak value that is overpredicted by as much as 25 %. These inaccuracies partially cancel when calculating the NO production rate, so that discrepancies in NO profiles are somewhat smaller. In view of these results, we can then conclude that the one-step global reaction NI (with rate determined by Eqs. 18 and 20) provides a reasonably good prediction for NO concentrations, although the two-step description NI-NII should be prefered in applications if increased accuracy is desired.

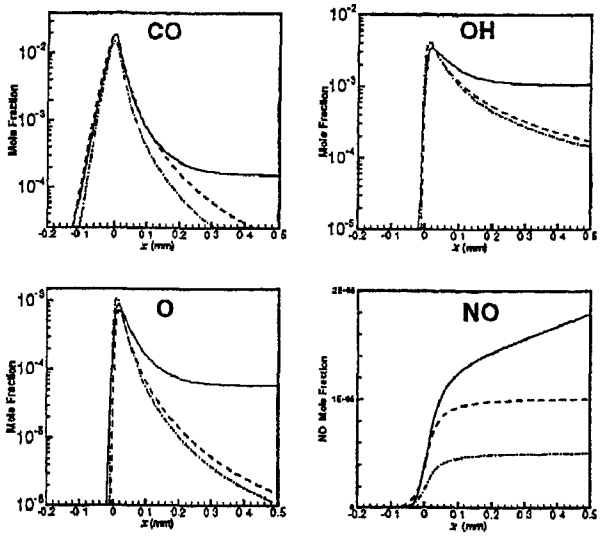

Figure 7: Mole fractions of radicals and pollutants across a premixed flame with $p = 18$ bar, $T_u = 800$ K and $\phi = 0.6$ as obtained with detailed chemistry (solid lines), with the reduced chemistry in the limit of irreversible radical recombination (dashed lines). and with the additional approximations $\alpha_2 = 1$, $\gamma = 0$ and $\omega_{NI} = k_{N18b}[O][N_2]$ (dot-dashed lines).

The Limit of Irreversible Radical Recombination

Neglecting the reverse of the radical-recombination reaction III', a simplification adopted in previous asymptotic analyses (Peters and Williams, 1987; Bui-Pham *et al.*, 1992) and also in the recent work of Li *et al.* (1999), leads to the reduced CO-oxidation rate previously given in Eq. 15. Since use of this more compact expression would somewhat reduce the effort required in computations, it is of interest to test the accuracy of the resulting approach. Thus, profiles of CO obtained by using Eq. 15 for the CO-oxidation rate are plotted in Fig. 7, along with profiles of radicals obtained from Eq. 13. The comparison with the results obtained with detailed chemistry indicates that the simplified rate adequately describes the peak value

and the initial decrease of the CO profiles, with the agreement being satisfactory over about two orders of magnitude in CO mole fraction. However, with irreversible radical recombination, the resulting description fails to reproduce the final equilibrium value, approaching instead a zero CO concentration far dowstream from the flame. A similar behavior is found for the radical profiles, with significant departures appearing at somewhat smaller distances.

The inaccuracies in the radical-pool description readily affect the nitrogen chemistry through the rate dependences on radical concentrations, an effect that is also exhibited in Fig. 7. As can be observed, the NO profile calculated in the limit of irreversible radical recombination exhibits large errors that are especially noticeable in the quasi-equilibrium region that extends downstream.

From the laminar results presented here it can be concluded that, although the assumption of irreversible radical recombination greatly simplifies the reduced kinetics, it introduces inaccuracies in predictions of CO and NO emissions that are in general too large. As can be expected, even larger errors arise when further chemistry simplifications are made. For instance, the additional approximations of negligible CO_2 consumption thorugh 17*b* ($\alpha_2 = 1$), slow radical recombination ($\gamma = 0$) and NO production exclusivelly controlled by the thermal path ($\omega_{NI} = k_{N1b}[O][N_2]$) are also tested in Fig. 7. Although the errors introduced through the simplifications of γ and α_2 in Eq. 15 partially compesate, a further decrease is seen in the resultant CO and radical mole fractions. The larger errors seen in the NO profile are only partially due to the reduced O concentration, with discrepancies being instead mainly attributable to the elementary reactions omitted in ω_{NI}.

SIMPLIFIED FORMULATION

The reduced kinetics developed above is designed to accurately describe combustion in LPP combustion chambers, enabling in particular the computation of CO and NO emissions. The associated numerical calculation of the flow field in the combustor requires the integration of the conservation equations for chemical species and energy, along with the continuity and momentum equations. In general, a model for turbulent transport must be incorporated in the conservation equations.

As a preliminary step to enable computations with the reduced kinetics proposed, we reformulate here the species and energy conservation equations in a simplified form that can be used as a starting point in modelling studies. In particular, the selected boundary conditions will be those of a propotypical gas-turbine combustion chamber. Thus, we consider a main feed stream that supplies a mixture of fuel and air, together with secondary feed streams that provide air to dilute the combustion products. For simplicity, we assume that the Lewis numbers of all the chemical species that remain out of steady state are unity (a very good approximation in view of the laminar flame calculations previously shown), and define a convective-diffusive diferential operator

$$L() = \frac{\partial}{\partial t}[\rho()] + \nabla \cdot [\rho \bar{v}()] - \nabla \cdot [\rho D_T \nabla()], \quad (21)$$

where ρ represents the density, $\bar{v}$ is the flow velocity and $D_T = \lambda/(\rho c_p)$ denotes the thermal diffusivity of the gas mixture, with λ and c_p representing its thermal conductivity and specific heat at constant pressure. In terms of this operator, the conservation equations for the reactive species corresponding to the reduced chemistry description I–II can be written as

$$L(\Gamma_{CH_4}) = -\omega_I, \quad (22)$$

$$L(\Gamma_{CO}) = \omega_I - \omega_{II}, \quad (23)$$

$$L(\Gamma_{CO_2}) = \omega_{II}, \quad (24)$$

$$L(\Gamma_{H_2O}) = 2\omega_I, \quad (25)$$

$$L(\Gamma_{O_2}) = -\frac{3}{2}\omega_I - \frac{1}{2}\omega_{II}, \quad (26)$$

where use is made of the variables $\Gamma_i = Y_i/W_i = [i]/\rho$, with Y_i and W_i denoting the mass fraction and molecular weight for chemical species i, respectively. To also describe NO production, the above equations must be supplemented with the conservation equations

$$L(\Gamma_{NO}) = \omega_{NI} \quad (27)$$

and

$$L(\Gamma_{N_2O}) = \omega_{NII}, \quad (28)$$

as follows from the nitrogen chemistry description. Note that the concentration of N_2, necessary to evaluate the rates of reactions NI and NII, can be either computed from the condition $\sum_i W_i\Gamma_i = 1$, or calculated by integrating the transport equation

$$L(\Gamma_{N_2}) = 0. \quad (29)$$

Similarly, the energy equation can be written for the thermal enthalpy $h_T = \int^T c_p dT$ as

$$L(h_T) = q_I\omega_I + q_{II}\omega_{II} - \nabla \cdot \bar{q}_R, \quad (30)$$

where the overall heats of reaction are related to the enthalpies of formation per mole of species i, h_i^o, by the equations $q_I = h_{CO}^o + 2h_{H_2O}^o - h_{CH_4}^o \simeq 124250$ cal/mole, and $q_{II} = h_{CO_2}^o - h_{CO}^o = 67700$ cal/mole. In the formulation, $\nabla \cdot \bar{q}_R$ represents the radiative heat loss per unit volumen. In writing Eq. 30, a low-Mach-number approximation has been employed, and unsteady pressure variations have been neglected along with the effect of the differences of the specific heat at constant pressure of each species from the mean c_p. To completely describe the reacting flow field, Eqs. 22–30 must be integrated together with the continuity and momentum equations with appropriate boundary and initial conditions.

Because of partial mixing between the fuel and the air, the conditions in the main feed stream are in general nonuniform, so that at the entrance of the combustor we find the reactant distributions $\Gamma_{CH_4} = \Gamma_{CH_4 m}$ and $\Gamma_{O_2} = \Gamma_{O_2 m}$, together with the nitrogen distribution $\Gamma_{N_2} = \Gamma_{N_2 m}$ and the thermal-enthalpy distribution $h_T = h_{Tm}$. If methane and air are used in generating the reactant mixture, then the local values of $\Gamma_{CH_4 m}$, $\Gamma_{O_2 m}$ and $\Gamma_{N_2 m}$ are related by the condition

$$\frac{\Gamma_{O_2 m}}{\Gamma_{O_2 a}} = \frac{\Gamma_{N_2 m}}{\Gamma_{N_2 a}} = 1 - \frac{\Gamma_{CH_4 m}}{W_{CH_4}^{-1}}, \quad (31)$$

where $\Gamma_{O_2 a} \simeq 0.23/W_{O_2}$ and $\Gamma_{N_2 a} \simeq 0.77/W_{N_2}$ are the values of the functions Γ_{O_2} and Γ_{N_2} in air. On the other hand, in the secondary feed streams, $\Gamma_{O_2} = \Gamma_{O_2 a}$, $\Gamma_{N_2} = \Gamma_{N_2 a}$, $\Gamma_{CH_4} = 0$ and $h_T = h_{T a}$. Also, appropriate boundary conditions in all streams are $\Gamma_{H_2O} = \Gamma_{CO_2} = \Gamma_{CO} = \Gamma_{NO} = \Gamma_{N_2O} = 0$. At the walls of the combustor, the nonpermeability condition yields $\nabla \Gamma_i \cdot \bar{n} = 0$ as the appropriate boundary condition for all species, where $\bar{n}$ is the unit vector normal to the wall. The boundary condition for the thermal enthalpy at the walls is in general more complicated and may require the detailed consideration of the heat conduction problem in the wall. In particular, the simple boundary condition $\nabla h_T \cdot \bar{n} = 0$ applies when the walls can be assumed to be adiabatic, while the assumption of isothermal walls leads to the constant boundary condition $h_T = h_{Tw}$.

In view of the above boundary conditions for CO and products, a first step to simplify the integration of Eqs. 22–30 follows from combining linearly Eqs. 23–25 to give

$$L(\Gamma_{CO} + \Gamma_{CO_2} - \frac{1}{2}\Gamma_{H_2O}) = 0, \tag{32}$$

an equation that can be readily integrated with the previously mentioned boundary conditions to give

$$\Gamma_{H_2O} = 2(\Gamma_{CO} + \Gamma_{CO_2}). \tag{33}$$

On the other hand, introducing the coupling functions

$$\begin{aligned} Z &= \frac{\Gamma_{CH_4} + \Gamma_{CO} + \Gamma_{CO_2}}{W_{CH_4}^{-1}} \\ &= \frac{\Gamma_{O_2 a} - \Gamma_{O_2} - \frac{3}{2}\Gamma_{CO} - 2\Gamma_{CO_2}}{\Gamma_{O_2 a}} \\ &= \frac{\Gamma_{N_2 a} - \Gamma_{N_2}}{\Gamma_{N_2 a}} \end{aligned} \tag{34}$$

and

$$H = \frac{h_T - h_{T a} - q_I \Gamma_{CO} - (q_I + q_{II})\Gamma_{CO_2}}{h_{T a}} \tag{35}$$

reduces the problem to that of integrating

$$L(\Gamma_{CH_4}) = -\omega_I, \tag{36}$$

$$L(\Gamma_{CO_2}) = \omega_{II}, \tag{37}$$

$$L(Z) = 0, \tag{38}$$

$$L(H) = -\nabla \cdot \bar{q}_R, \tag{39}$$

$$L(\Gamma_{NO}) = \omega_{NI} \tag{40}$$

$$L(\Gamma_{N_2O}) = \omega_{NII} \tag{41}$$

with boundary conditions $\Gamma_{CH_4} = \Gamma_{CH_4 m}$, $\Gamma_{CO_2} = \Gamma_{NO} = \Gamma_{N_2O} = 0$, $Z = Z_m = \Gamma_{CH_4 m}/W_{CH_4} = (\Gamma_{O_2 a} - \Gamma_{O_2 m})/\Gamma_{O_2 a} = (\Gamma_{N_2 a} - \Gamma_{N_2 m})/\Gamma_{N_2 a}$ and $H = H_m = (h_{T m} - h_{T a})/h_{T a}$ in the main feed stream, and $\Gamma_{CH_4} = \Gamma_{CO_2} = \Gamma_{NO} = \Gamma_{N_2O} = Z = H = 0$ in the secondary feed streams. At the walls, the variable Z satisfies $\nabla Z \cdot \bar{n} = 0$, while the boundary condition for H is more complicated, reducing to $\nabla H \cdot \bar{n} = 0$ when adiabatic walls are considered and to $H = [(h_{Tw} - h_{T a}) - q_I(Z/W_{CH_4} - \Gamma_{CH_4}) - q_{II}\Gamma_{CO_2}]/h_{T a}$ in the case of isothermal walls. Note that the definition of Z shown in Eq. 34 is motivated by the relationship between the fuel and air content in the feed stream displayed in Eq. 31.

In the particular case of perfect mixing, the boundary conditions for Z and H in the main stream reduce to constant values that can be used to redefine normalized variables $\bar{Z} = Z/Z_m$ and $\bar{H} = H/H_m$, so that $\bar{Z} = \bar{H} = 1$ in the main stream. A further simplification arises when adiabatic walls are considered and radiation is neglected, a case for which Eq. 40 can be replaced by $H = H_m Z/Z_m$, which in turn reduces to $H = 0$ if $h_{T m} = h_{T a}$.

REFERENCES

Baulch, D. L., Cobos, C. J., Cox, R. A., Frank, P., Hayman, G., Just, Th., Kerr, J. A., Murrells, T., Pilling, M. J., Troe, J., Walker, R. W., and Warnatz, J. (1994). Summary Table of Evaluated Kinetic Data for Combustion Modelling: Supplement 1, *Combust. and Flame* 98, pp. 59-79.

Bui-Pham, M., Seshadri, K. and Williams, F. A. (1992). The Asymptotic Structure of Premixed Methane-Air Flames with Slow CO Oxidation, *Combust. Flame*, 89, pp. 343–362.

Hewson, J., and Bollig, M. (1996) Reduced Mechanisms for NO_x Emissions from Hydrocarbon Diffusion Flames, *Twenty-Sixth Symposium (International) on Combustion*, The Combustion Institute, Pittsburgh, PA, 1996, pp 2171–2179.

Li, S. C., Williams, F. A., and Gebert, K. (1999), A Simplified, Fundamentally Based Method for Calculating NOx Emissions in Lean Premixed Combustors, *Combust. Flame*, to appear.

Liñán, A., Sánchez, A. L., Lépinette, A., Bollig, M., and Lázaro, B. (1999). The Reduced Kinetic Description of Lean Premixed Combustion, in preparation.

Peters, N. and Rogg, B. (Eds.) (1993) *Reduced Kinetic Mechanisms for Applications in Combustion Systems*, Lecture Notes in Physics m15, Springer-Verlag.

Peters, N. and Williams, F. A. (1987). The Asymptotic Structure of Stoichiometric Methane Air Flames, *Combust. Flame*, 68 pp. 185–207.

Pitsch, H., and Bollig, M. (1994) *"FlameMaster*, A Computer Code for Homogeneous and One-Dimensional Laminar Flame Calculations", Institut für Technische Mechanik, RWTH-Aachen.

Swaminathan, N. and Bilger, R. W. (1997). Direct Numerical Simultation of Turbulent Nonpremixed Hydrocarbon Reaction Zones Using a Two-Step Reduced Mechanism. *Comb. Sci. Technol.* 127, pp. 167–196.